OL | Organic Letters

pubs.acs.org/OrgLett

Letter

Reductive Dimerization of Macrocycles Activated by BBr_3

Monika Kijewska, Miłosz Siczek, and Miłosz Pawlicki*

Cite This: *Org. Lett.* 2021, 23, 3652−3656

Read Online

ACCESS | Metrics & More | Article Recommendations | Supporting Information

ABSTRACT: A macrocyclic motif composed of carbazole and pyridine subunits linked by a carbonyl bridge (C═O) forms a skeleton with a peripheral reactivity that leads to a pinacol-like coupling activated by BBr_3, eventually entrapping a substantially elongated C−C bond. Slightly modified conditions lead to the efficient transformation of the C═O unit to a CH_2 linker that, after exposure to air, gives a dimeric molecule with multiple bonds between two macrocyclic units, as documented in spectroscopy and X-ray analysis.

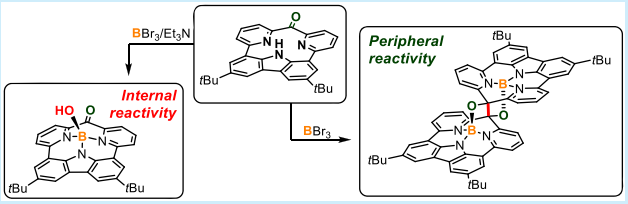

The precise design of novel structural motifs with envisioned properties remains the central theme of logic in chemistry. Such structures, apart from potential applications, often provide platforms for the exploration and development of novel concepts in fundamental aspects such chemical bonding or potential reactivity. The formation of unsaturated macrocycles that keep local conjugation opens a specific set of options for postsynthetic transformation[1] in addition to opening new frontiers of reactivity. Pyridine-incorporated structures are reported as motifs where both types of behavior have been observed to show global conjugation[2] or to keep local effects[3] and postsynthetic modifications.[4] The coordination plays an important role in macrocycles, strongly modulating the observed behavior, including the formation of dimeric motifs driven by coordination[5] that can lead to *μ-oxo*-dimers.[6] The linking of two monomeric macrocycles into covalently bound skeletons was realized via a transition-metal catalyst[7] or with a standard condensation approach.[8] As reported to date, the triheterocyclic/carbocyclic systems linked with carbon bridges form a perfect environment for binding boron(III), which effectively interacts with carbon[9] or nitrogen[10] but also stabilizes a global effect of antiaromatic delocalization.[11] However, the triangular shape of the macrocyclic environment that is predefined for binding boron(III) can create different sets of donors very efficiently, utilizing the electron deficiency of the central ion and leading to the intriguing modulation of the final skeleton, while the global delocalization is disturbed and the local influences are crucial.[1,4] Following these observations, here we report the studies of the precisely designed and synthesized macrocycle constructed of heterocyclic subunits linked with a carbonyl (C═O) unit, showing two reactivities distinguished as *internal* and *peripheral*.

In our approach, we applied Suzuki−Miyaura coupling as a versatile tool for the formation of *π*-extended molecules,[9−12] and it is also applicable for the synthesis of macrocycles.[13] Both required reagents **1** and **2** were obtained as previously described[14,15] and subjected to palladium-catalyzed coupling (Scheme 1, path *a*), eventually giving macrocycle **3** in 20% yield. As documented in the ^{1}H NMR analysis (Figure 1A), **3** remains locally aromatic according to the magnetic criterion,[18] with a downfield-shifted line of H(3,20) at *δ* 8.18. The recorded spectroscopic properties are consistent with rather negligible macrocyclic delocalization compared with other structures of similar size[9−12] but also containing pyridine and carbazole.[16] The lack of macrocyclic delocalization is consistent with the presence of the carbonyl linker documented in the ^{13}C NMR (*δ* 187.1) that efficiently blocks the delocalization. The final structure shows a strongly downfield-shifted internal proton of the NH group (*δ* 18.48), proving the proximity of three nitrogen centers and a strong hydrogen bond responsible for the significant deshielding of hydrogen.[4,17] The presence of three nitrogen donors in a confined macrocyclic construction similar to triphyrins creates a perfect environment for small cations such as boron(III).[10,11] The reaction of **3** with boron(III) tribromide (BBr_3) in the presence of triethyl amine (Et_3N), applied as a neutralizing medium, showed the *internal* variant of reactivity (Scheme 1, path *b*). The LC-MS analysis of the reaction mixture showed an *m*/*z* peak at 486.2330, consistent with that of monomeric skeleton **4a** with a hydroxy axial ligand isolated in 28% yield. A deeper analysis of the reaction mixture showed the presence of doubly charged motif at *m*/*z* 477.2288 (+2), eventually assigned to *μ-oxo*-dimer **5** (Scheme 1). The formation of oxygen-bridged structures was reported for

Received: March 26, 2021
Published: April 15, 2021

Scheme 1. Synthetic Approach[a]

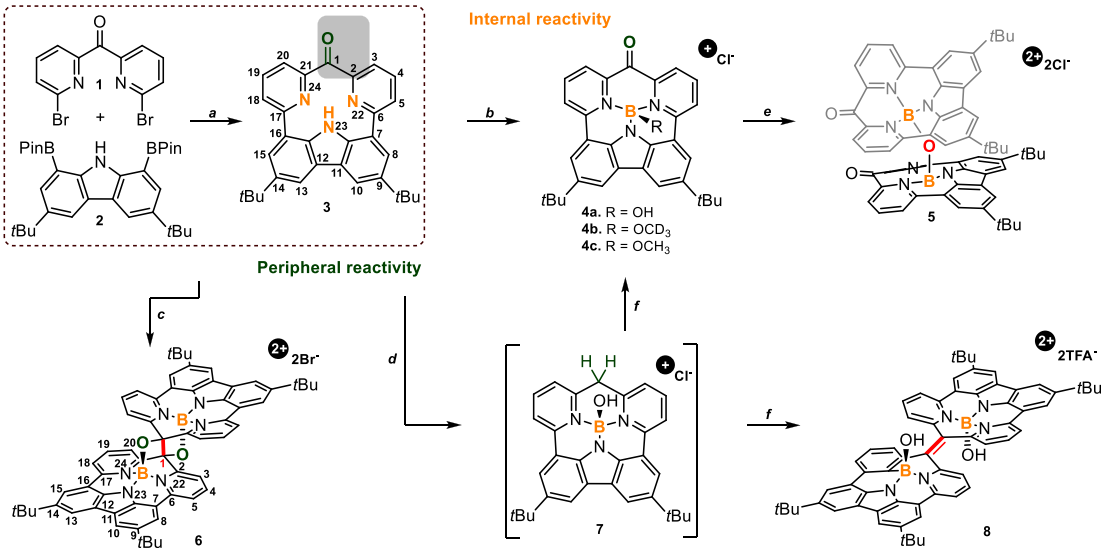

[a]Conditions: (a) **1** (1 equiv), **2** (1 equiv), $Pd(PPh_3)_4$ (0.1 equiv), K_2CO_3 (3 equiv), KF (4 equiv), toluene/DMF, 110 °C, 72 h. (b) BBr_3 (10 equiv), Et_3N (13 equiv), toluene, reflux, Ar, 2 h. (c) BBr_3 (10 equiv), toluene, reflux, Ar, 2 h. (d) BBr_3 (10 equiv), *o*-dichlorobenzene, reflux, Ar, 2 h. (e) Zn(Hg), $CDCl_3$, Ar, 24 h (incubation 12 h, 60°C). (f) O_2, 24 h.

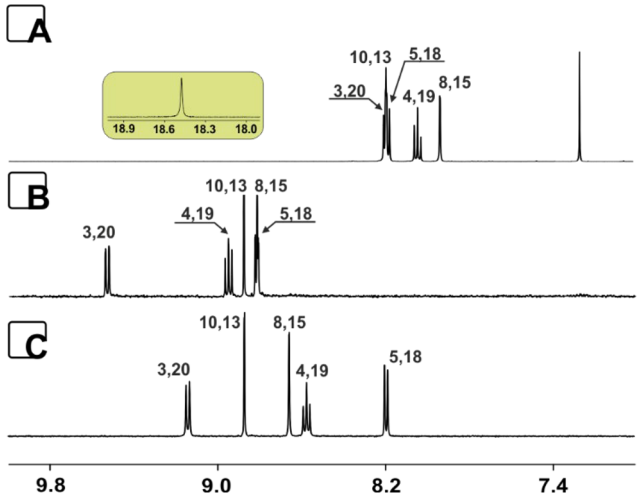

Figure 1. ^{1}H NMR spectra of **3** (A, chloroform-*d*), **4a** (B, acetone-d_6), and **6** (C, acetone-d_6) (600 MHz, 300 K).

different cations including transition metals[6a] and metalloids.[6b] As documented, the formation of **5** was observed in the presence of Et_3N, which activates the axial hydroxy ligand at the boron(III) center. Importantly, **5** can be also directly obtained from **4a** (Scheme 1, path *e*) in 45% yield. The insertion of B(III) does not change the local character of aromaticity observed in **4a,** as documented by ^{1}H NMR (Figure 1B). The presence of a carbonyl unit in both derivatives **4a** and **5** was proved by the ^{13}C chemical shifts observed at δ 177.0 and δ 176.1, respectively. **4** showed a specific pattern of pyridine resonances with a significantly downfield-shifted line of H(3,20) (δ 9.54 (**4a**)), whereas **5** relocated the pyridine resonances H(3,20) up-field to δ 9.16 (Figure S39).

While dissolved in acetone-d_6, both positively charged boron(III) complexes **4** and **5** efficiently accommodate one molecule of acetone via an enolation of acetone that acts as a nucleophile toward the carbonyl unit, forming an sp^3-hybridized carbon and showing peripheral reactivity. The ^{13}C NMR spectra showed the formation of a tetrahedral carbon for the conversion of **4a** (δ 75.9 **4**-*Ac*), whereas the reaction of **5** gave two types of carbons (δ 176.1 and δ 75.4), proving the accommodation of one molecule of acetone in **5**-*Ac* (Figure 2). The significant difference in both positions (Figure S46) is consistent with keeping the sp^2 carbonyl in one subunit and changing the hybridization to sp^3 in the second one.

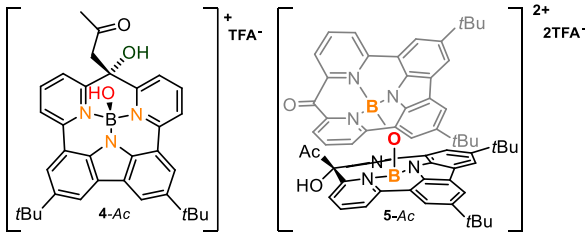

Figure 2. Acetone adducts of **4**-*Ac* and **5**-*Ac*.

The X-ray analysis performed for **3** confirmed steric confinements resulting in the proximity of three nitrogen donors (Figure 3A), and the distances observed within the coordination cavity are consistent with a strong N−H···N hydrogen bond responsible for the substantial downfield shift of H(23) in the ^{1}H NMR spectrum.[4,17] Crystal structures confirmed the presence of carbonyl units in **3** and **4a** (Figure 3A,B; C(1)−O(1) bond lengths 1.223(3) and 1.217(6) Å, respectively) and the tetrahedral geometry of C1 in **4a**-*Ac* (Figure 3C). The boron(III) environment in **4a** and **4a**-*Ac* showed the pyramidal organization of donors with characteristic bond lengths (Figure 3) and a hydroxyl group as an axial ligand. The crystal structure of **5**-*Ac* (see the Supporting Information) showed the presence of both types of subunits, confirming the formation of another C−C bond (Figure S105).

The reactivity at the carbonyl unit observed in **4** and **5** consistently suggested the potential toward the formation of

https://doi.org/10.1021/acs.orglett.1c01047
Org. Lett. 2021, 23, 3652−3656

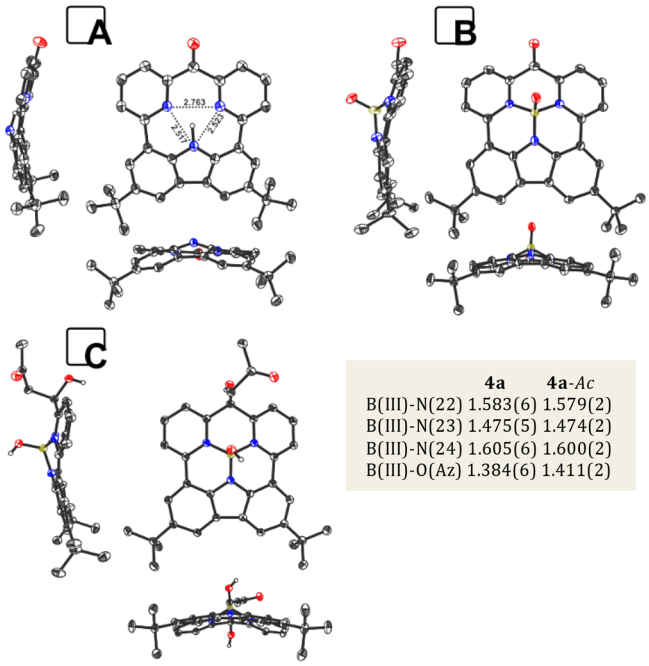

Figure 3. Molecular structures of **3** (A, thermal ellipsoids present 30% probability), **4a** (B, thermal ellipsoids present 50% probability), and **4**-*Ac* (C, thermal ellipsoids present 50% probability). Counter ions, solvents, and hydrogen atoms are removed for clarity.

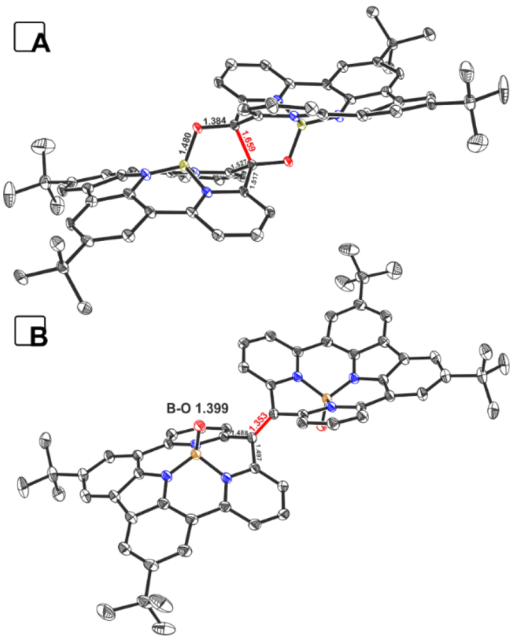

Figure 4. Crystal structures of **6** (A) and **8** (B) (thermal ellipsoids at 30% probability). Counter ions, solvents, and hydrogen atoms are removed for clarity.

new carbon−carbon bonds, opening a path for the *peripheral* reactivity (Scheme 1). Carbonyl units are effective substrates for reactions like pinacol coupling, which consists of a reduction step crucial for the formation of a C−C bond and requiring the employment of transition metals.[7,20] The reaction of **3** with boron(III) tribromide (BBr_3, *excess*) without triethyl amine (Scheme 1, path *c*) gave a product that showed a doubly charged peak at m/z = 469.2311 as a major component accompanied by a substantially smaller amount of **4a** and a second doubly charged structure with an m/z peak at 470.2381 (Figure S80).

The isotopic patterns recorded for both doubly charged fractions were consistent with the presence of two boron(III) cations. The NMR analysis with substantially different patterns of resonances in the ^{1}H spectrum compared with **4a** with noticeably upfield-relocated pyridine lines (Figure 1C) and the presence of an sp^3 carbon (^{13}C δ 84.5, Figure S56) connected to a heteroatom allowed us to suggest the expected structure for the major fraction to be **6** (Scheme 1) stabilizing a pinacol motif. The second dimeric structure, eventually identified as **8** (Scheme 1), showed a substantially different spectroscopic pattern consistent with a double bond linking two macrocyclic subunits. The X-ray analysis of **6** (Figure 4A) confirmed the conclusions derived from spectroscopic data. An sp^3-hybridized carbon in a pinacol-like motif that coordinates to boron(III) centers (Figure 3A) was observed. The boron(III) environment (B−N(22) (1.573(6) Å), B−N(23) (1.432(6) Å) and B−N(24) 1.569(6) Å) was comparable to that for **4a** and also that for other B(III)−N interactions. Both macrocyclic subunits are linked via two B−O−C connections that keep two sp^3-hybridized C(1) atoms in an orientation that forms a C−C bond with a length of 1.659(6) Å, which is noticeably longer than regular sp^3−sp^3 interaction.[19] The Wiberg index calculated for the elongated C−C bond (0.8416) confirmed the decreased bond order, consistent with the observed length. The crystal structure of **8** (Figure 4B) confirmed the presence of a significantly shorter C−C bond (1.354(4) and 1.344(4) Å for two independent molecules in a crystal cell) characteristic of a double interaction. Both dimeric structures were stable and could be kept in solution for several weeks while protected from the air. Unprotected from the air, the sample of **6** in methanol(methanol-d_4) or the mixture of acetonitrile/water quantitatively converted to **4b**(**4c**) or **4a**, respectively (Figures S89 and S90), which can explain the presence of **4a** in the reaction mixture. Under the same conditions, **8** remained intact.

The UV−vis properties consistently support the limited global delocalization, showing a negligible change when comparing all derivatives (Figure S99). The NH dynamic substantially affects the emission[21] that is not observed for **3** but is detectable for boron(III) complexes (Figure S103) and recorded at λ = 506 (**4a**), 510 (**6**), and 511 nm (**8**).

The plausible mechanism leading to **6** involves the dimerization of monomers **3** activated by BBr_3, leading to a tetracationic skeleton (Scheme 2), followed by a reductive C−C bond formation. The applied conditions do not introduce any obvious source of electrons; however, Br^- was reported as an electron-transfer medium acting as a reducing agent in multicharged skeletons.[23a] Thus an excess of bromide anions plays a crucial role in dimerization, and the observed behavior shows the influence of the introduction of positive charges to the system followed by the electron transfer that reflects some analogy to the proton-coupled electron transfer (PCET).[23]

While looking at **6** and **8**, it can be concluded that both dimeric structures can be interconverted by a redox process. Nevertheless, all reduction attempts to convert **6** to **8** were met with failure, suggesting a separate path. Because we did not observe the formation of **8** under the first conditions (with Et_3N), we decided to modify the synthetic approach leading to **6** by extending the reaction time to 12 h of reflux in toluene. This gave **6** as a dominating component, accompanied by **4a** and **8**. The LC-MS analysis showed an additional mono-

https://doi.org/10.1021/acs.orglett.1c01047
Org. Lett. 2021, 23, 3652−3656

Scheme 2. Potential Mechanism in Two Variants for the Reductive Coupling of Carbonyls Activated with BBr_3[a]

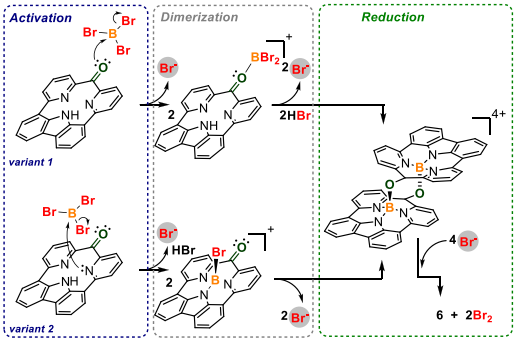

[a] *t*Bu is not present for clarity.

cationic compound at an *m*/*z* signal of 472.2553 that vanishes after exposure to air with a simultaneous increase in the amount of **4a** and **8** (Figure S95), suggesting a correlation between these species. By using a highly boiling solvent (*o*-dichlorobenzene) for the same process (Scheme 1, path *d*), we observed the formation of 472.2553 as a single product that was eventually assigned to the reduced skeleton **7** (Scheme 1) containing a $-CH_2-$ bridge instead of a carbonyl unit (Figures S96 and S97). As reported by Newkome and coworkers, a $-CH_2-$ group flanked by two pyridines is highly reactive and leads to dimerization,[16d,22] similar to our observations where **7** converts to **8** (Scheme 1, path *f*). A potential approach to reduce the carbonyl unit to form **7** can be presented with similarities to the classic Clemmensen reduction (Scheme S2) with the involvement of Br^- as an electron-transfer agent. Both reductive processes leading to **6** and **7** should have similar origins, as both derivatives were observed under similar conditions. Thus while looking at the optimized conditions, we can say that depending on the presence of triethyl amine, the predominant formation of monomeric (with Et_3N) or dimeric (without Et_3N) boron(III) complexes can be observed. In addition, the different reaction temperatures can be applied to form either **6** or **8** (via **7**).

In conclusion, a rationally obtained macrocycle armed with peripherally located carbonyl functionality undergoes a BBr_3-activated conversion that, depending on the applied conditions, gives monomeric or dimeric boron(III) complexes. The dimerization gives a pinacol-like coupling of two subunits with the stabilization of the elongated C−C bond, as documented in the X-ray analysis. With slightly modified conditions, two macrocycles form a double bond that bridges both subunits. The presented approach, with the possibility of controlling the type of reactivity, shows that the precise design of the skeleton opens the potential for controlled conversion to highly appreciated motifs linking π-extended systems into more complex structures. Further experiments toward this reactivity are under way in our lab.

■ ASSOCIATED CONTENT

Supporting Information

The Supporting Information is available free of charge at https://pubs.acs.org/doi/10.1021/acs.orglett.1c01047.

General methods, synthesis, and characterization of all compounds (PDF)

Accession Codes

CCDC 2054315−2054319 contain the supplementary crystallographic data for this paper. These data can be obtained free of charge via www.ccdc.cam.ac.uk/data_request/cif, or by emailing data_request@ccdc.cam.ac.uk, or by contacting The Cambridge Crystallographic Data Centre, 12 Union Road, Cambridge CB2 1EZ, UK; fax: +44 1223 336033.

■ AUTHOR INFORMATION

Corresponding Author

Miłosz Pawlicki − *Department of Chemistry, University of Wrocław, 50383 Wrocław, Poland; Faculty of Chemistry, Jagiellonian University, 30387 Kraków, Poland;* orcid.org/0000-0002-8249-0474; Email: pawlicki@chemia.uj.edu.pl

Authors

Monika Kijewska − *Department of Chemistry, University of Wrocław, 50383 Wrocław, Poland;* orcid.org/0000-0001-6227-7169

Miłosz Siczek − *Department of Chemistry, University of Wrocław, 50383 Wrocław, Poland*

Complete contact information is available at: https://pubs.acs.org/10.1021/acs.orglett.1c01047

Notes

The authors declare no competing financial interest.

■ ACKNOWLEDGMENTS

Financial support from the National Science Centre, Poland (2016/23/B/ST5/01186) is kindly acknowledged. The Wrocław Supercomputer Centre (KDM WCSS) is kindly acknowledged for sharing computation resources necessary for DFT calculations. We thank Andrzej Reszka (Shim-Pol, Poland) for providing the Shimadzu IT-TOF instrument.

■ REFERENCES

(1) (a) Suzuki, M.; Osuka, A. Cross-Bridging Reaction of 5,20-Diethynyl Substituted Hexaphyrins to Vinylene-Bridged Hexaphyrins. *J. Am. Chem. Soc.* **2007**, *129*, 464−465. (b) Pawlicki, M.; Bykowski, D.; Szterenberg, L.; Latos-Grażyński, L. From 21,23-dioxaporphyrin to a 3-pyranone dioxacorrole skeleton: the Achmatowicz rearrangement in the porphyrin frame. *Angew. Chem., Int. Ed.* **2012**, *51*, 2500−2504. (c) Umetani, M.; Tanaka, T.; Kim, T.; Kim, D.; Osuka, A. Double Ring Expansion from an Aromatic [18]Porphyrin(1.1.1.1) to an Antiaromatic [20]Porphyrin(2.1.2.1). *Angew. Chem., Int. Ed.* **2016**, *55*, 8095−8099.

(2) (a) Myśliborski, R.; Hurej, K.; Pawlicki, M.; Latos-Grażyński, L. Inversion Triggered by Protonation-A Rubyrin with Embedded *α,β'*-Pyridine Moieties. *Angew. Chem., Int. Ed.* **2018**, *57*, 16866−16870. (b) Zhang, Z.; Cha, W.-Y.; Williams, N. J.; Rush, E. L.; Ishida, M.; Lynch, V. M.; Kim, D.; Sessler, J. L. Cyclo[6]pyridine[6]pyrrole: A Dynamic, Twisted Macrocycle with No Meso Bridges. *J. Am. Chem. Soc.* **2014**, *136*, 7591−7594. (c) Setsune, J.; Watanabe, K. Cryptand-like Porphyrinoid Assembled with Three Dipyrrylpyridine Chains: Synthesis, Structure, and Homotropic Positive Allosteric Binding of Carboxylic Acids. *J. Am. Chem. Soc.* **2008**, *130*, 2404−2405. (d) Liu, L.; Hu, Z.; Zhang, F.; Liu, Y.; Xu, L.; Zhou, M.; Tanaka, T.; Osuka, A.; Song, J. Benzene- and pyridine-incorporated octaphyrins with different coordination modes toward two Pd^{II} centers. *Nat. Commun.* **2020**, *11*, 6206.

(3) (a) Listkowski, A.; Jędrzejewski, P.; Kijak, M.; Nawara, K.; Kowalska, P.; Luboradzki, R.; Waluk, J. Antiaromatic or Non-aromatic? 21H,61H-2,6(2,5)-Dipyrrola-1,5(2,6)-dipyridinacyclo octa-

phane-3,7-diene: a Porphycene Derivative with 4N π Electrons. *J. Phys. Chem. A* **2019**, *123*, 2727−2733. (b) Newkome, G. R.; Joo, Y. J.; Theriot, K. J.; Fronczek, F. R. Convenient Synthesis and Structural Aspects of 1,3,5-Tri[2,6]pyridacyclohexaphane-2,4,6-trione and Precursors. *J. Am. Chem. Soc.* **1986**, *108*, 6074−6075.

(4) Klajn, J.; Stawski, W.; Chmielewski, P. J.; Cybińska, J.; Pawlicki, M. A Route to a Cyclobutane-Linked Double-Looped System via a Helical Macrocycle. *Chem. Commun.* **2019**, *55*, 4558−4561.

(5) Wojaczyński, J.; Latos-Grażyński, L. Poly-and oligometalloporphyrins associated through coordination. *Coord. Chem. Rev.* **2000**, *204*, 113−171.

(6) (a) Pawlicki, M.; Latos-Grażyński, L. Iron Complexes of 5,10,15,20-Tetraphenyl-21-oxaporphyrin. *Inorg. Chem.* **2002**, *41*, 5866−5873. (b) Sorokin, A. B. Recent progress on exploring μ-oxo bridged binuclear porphyrinoid complexes in catalysis and material science. *Coord. Chem. Rev.* **2019**, *389*, 141−160.

(7) Hiroto, S.; Miyake, Y.; Shinokubo, H. Synthesis and Functionalization of Porphyrins through Organometallic Methodologies. *Chem. Rev.* **2017**, *117*, 2910−3043.

(8) Pawlicki, M.; Morisue, M.; Davis, N. K. S.; McLean, D. G.; Haley, J. E.; Beuerman, E.; Drobizhev, M.; Rebane, A.; Thompson, A. L.; Pascu, S. I.; Accorsi, G.; Armaroli, N.; Anderson, H. L. Engineering conjugation in para-phenylene-bridged porphyrin tapes. *Chem. Sci.* **2012**, *3*, 1541−1547.

(9) Stawski, W.; Hurej, K.; Skonieczny, J.; Pawlicki, M. Organoboron Complexes in Edge-Sharing Macrocycles: The Triphyrin(2.1.1) - Tetraphyrin(1.1.1.1) Hybrid. *Angew. Chem., Int. Ed.* **2019**, *58*, 10946−10950.

(10) (a) Kuzuhara, D.; Xue, Z.; Mori, S.; Okujima, T.; Uno, H.; Aratani, N.; Yamada, H. Synthesis and properties of boron complexes of [14]triphyrins(2.1.1). *Chem. Commun.* **2013**, *49*, 8955−8957. (b) Pawlicki, M.; Hurej, K.; Szterenberg, L.; Latos-Grażyński, L. Synthesis and Switching the Aromatic Character of Oxatriphyrins(2.1.1). *Angew. Chem., Int. Ed.* **2014**, *53*, 2992−2996.

(11) (a) Pawlicki, M.; Garbicz, M.; Szterenberg, L.; Latos-Grażyński, L. Oxatriphyrins(2.1.1) incorporating an ortho-phenylene motif. *Angew. Chem., Int. Ed.* **2015**, *54*, 1906−1909. (b) Bartkowski, K.; Dimitrova, M.; Chmielewski, P. J.; Sundholm, D.; Pawlicki, M. Aromatic and Antiaromatic Pathways in Triphyrin(2.1.1) Annelated with Benzo[*b*]heterocycles,. *Chem. - Eur. J.* **2019**, *25*, 15477−15482. (c) Bartkowski, K.; Pawlicki, M. (Aza)Acenes Share the C2 Bridge with (Anti)Aromatic Macrocycles: Local vs. Global Delocalization Paths. *Angew. Chem., Int. Ed.* **2021**, *60*, 9063−9070.

(12) Gopee, H.; Kong, X.; He, Z.; Chambrier, I.; Hughes, D. L.; Tizzard, G. J.; Coles, S. J.; Cammidge, A. N. Expanded Porphyrin-like Structures Based on Twinned Triphenylenes. *J. Org. Chem.* **2013**, *78*, 9505−9511.

(13) Sathish Kumar, B.; Pati, N. N.; Jose, K. V. J.; Panda, P. K. Synthetic access to calix[3]pyrroles via meso-expansion: hosts with diverse guest chemistry. *Chem. Commun.* **2020**, *56*, 5637−5640.

(14) Li, X.; Gibb, C. L. D.; Kuebel, M. E.; Gibb, B. C. Two new ligands for carbonic anhydrase mimicry. *Tetrahedron* **2001**, *57*, 1175−1182.

(15) (a) Arnold, L.; Norouzi-Arasi, H.; Wagner, M.; Enkelmann, V.; Müllen, K. A porphyrin related macrocycle from carbazole and pyridine building blocks: synthesis and metal coordination. *Chem. Commun.* **2011**, *47*, 970−972. (b) Maeda, Ch.; Yoneda, T.; Aratani, N.; Yoon, M.-C.; Lim, J. M.; Kim, D.; Yoshioka, N.; Osuka, A. Synthesis of Carbazole-Containing Porphyrinoids by a Multiple Annulation Strategy: A Core-Modified and π-Expanded Porphyrin. *Angew. Chem., Int. Ed.* **2011**, *50*, 5691−5694.

(16) (a) Newkome, G. R.; Nayak, A.; Sauer, J. D.; Mattschei, P. K.; Watkins, S. F.; Fronczek, F.; Benton, W. H. Molecular Inclusion Compounds. Ketonic and Spiro Heteromacrocycles Possessing 2,6-Pyridino Moieties Connected by a Carbon-Oxygen and/or-Sulfur Bridge. *J. Org. Chem.* **1979**, *44*, 3816−3826. (b) Newkome, G.; Taylor, R. M. C. R.; Fronczek, F. R.; Delord, T. J. Syntheses, Conformational Studies, and Reactions of Heteromacrocycles. Bis(2-pyridyl) Ketone Derivatives. *J. Org. Chem.* **1984**, *49*, 2961−2971. (c) Newkome, G. R.; Joo, Y. J.; Fronczek, F. R. Synthesis of a Pyridine-containing Xanthoporphinogen-type Model. An Entrance to Heterocalixarenes. *J. Chem. Soc., Chem. Commun.* **1987**, 854−856. (d) Newkome, G. R.; Joo, Y. J.; Evans, D. W.; Fronczek, F. R.; Baker, G. R. 1,3,5-Tri[2,6]pyridacyclohexaphane-2,4,6-trione Ketals: Synthesis, Structural Analysis, and Complexation. *J. Org. Chem.* **1990**, *55*, 5714−5719.

(17) Pawlicki, M.; Szterenberg, L.; Latos-Grażyński, L. 5,10,15-Triaryl-21,23-dioxacorrole and Its Isomer with a Protruding Furan Ring. *J. Org. Chem.* **2002**, *67*, 5644−5653.

(18) Pawlicki, M.; Latos-Grażyński, L. Aromaticity switching in porphyrinoids. *Chem. - Asian J.* **2015**, *10*, 1438−1451.

(19) Nakakuki, Y.; Hirose, T.; Sotome, Y.; Miyasaka, H.; Matsuda, K. Hexa-peri-hexabenzo[7]helicene: Homogeneously π-Extended Helicene as a Primary Substructure of Helically Twisted Chiral Graphenes. *J. Am. Chem. Soc.* **2018**, *140*, 4317−4326.

(20) (a) Schreiner, P. R.; Chernish, L. V.; Gunchenko, P. A.; Tikhonchuk, E. Y.; Hausmann, H.; Serafin, M.; Schlecht, S.; Dahl, J. E. P.; Carlson, R. M. K.; Fokin, A. A. Overcoming lability of extremely long alkane carbon−carbon bonds through dispersion forces. *Nature* **2011**, *477*, 308−311. (b) Kammermeier, S.; Jones, P. G.; Herges, R. [2 + 2] Cycloaddition Products of Tetradehydro-dianthracene: Experimental and Theoretical Proof of Extraordinary Long C-C Single Bonds. *Angew. Chem., Int. Ed. Engl.* **1997**, *36*, 1757−1760. (c) Tanaka, K.; Takamoto, N.; Tezuka, Y.; Kato, M.; Toda, F. Preparation and structural study of naphtho- and anthrocyclobutene derivatives which have extremely long C−C bonds. *Tetrahedron* **2001**, *57*, 3761−3767. (d) Ishigaki, Y.; Shimajiri, T.; Takeda, T.; Katoono, R.; Suzuki, T. Longest C−C Single Bond among Neutral Hydrocarbons with a Bond Length beyond 1.8 Å. *Chem.* **2018**, *4*, 795−806. (e) Li, J.; Pang, R.; Li, Z.; Lai, G.; Xiao, X.-Q.; Müller, T. Exceptionally Long C-C Single Bonds in Diamino-o-carborane as Induced by Negative Hyperconjugation. *Angew. Chem., Int. Ed.* **2019**, *58*, 1397−1401. (f) Mandal, N.; Pal, A. K.; Gain, P.; Zohaib, A.; Datta, A. Transition-State-like Planar Structures for Amine Inversion with Ultralong C−C Bonds in Diamino-o-carborane and Diamino-o-dodecahedron. *J. Am. Chem. Soc.* **2020**, *142* (11), 5331−5337. (g) Shimajiri, T.; Suzuki, T.; Ishigaki, Y. Flexible C−C Bond: Reversible Expansion, Contraction, Formation, and Scission of Extremely Elongated Single Bonds. *Angew. Chem., Int. Ed.* **2020**, *59*, 22252−22257.

(21) (a) Sobolewski, A. L.; Gil, M.; Dobkowski, J.; Waluk, J. On the Origin of Radiationless Transitions in Porphycenes. *J. Phys. Chem. A* **2009**, *113*, 7714−7716. (b) Iima, Y.; Kuzuhara, D.; Xue, Z.-L.; Akimoto, S.; Yamada, H.; Tominaga, K. Time-resolved fluorescence spectroscopy study of excited state dynamics of alkyl- and benzo-substituted triphyrin(2.1.1). *Phys. Chem. Chem. Phys.* **2014**, *16*, 13129−13135. (c) Hurej, K.; Stawski, W.; Latos-Grażyński, L.; Pawlicki, M. meso-N-Pyrrole as a Versatile Substituent Influencing the Optical Properties of Porphyrin. *Chem. - Asian J.* **2016**, *11*, 3329−3333. (d) Kim, K. S.; Lim, J. M.; Myśliborski, R.; Pawlicki, M.; Latos-Grażyński, L.; Kim, D. Origin of Ultrafast Radiationless Deactivation Dynamics of Free-Base Subpyriporphyrins. *J. Phys. Chem. Lett.* **2011**, *2*, 477−481.

(22) Klemm, E.; Klemm, D.; Hörhold, H. H. Dehydrierende Dimerisierung von 2-(4-Nitrobenzyl)- und 2-(2,4-Dinitrobenzyl)-pyridinen. *Synthesis* **1977**, *1977*, 342.

(23) (a) Sarma, T.; Kim, G.; Sen, S.; Cha, W.-Y.; Duan, Z.; Moore, M. D.; Lynch, V. M.; Zhang, Z.; Kim, D.; Sessler, J. L. Proton-Coupled Redox Switching in an Annulated π-Extended Core Modified Octaphyrin. *J. Am. Chem. Soc.* **2018**, *140*, 12111−12119. (b) Gentry, E. C.; Knowles, R. R. Synthetic Applications of Proton-Coupled Electron Transfer. *Acc. Chem. Res.* **2016**, *49*, 1546−1556.

https://doi.org/10.1021/acs.orglett.1c01047
Org. Lett. 2021, 23, 3652−3656